

Sleptons at a First Muon Collider

Frank E. Paige

Physics Department
Brookhaven National Laboratory
Upton, NY 11973 USA

ABSTRACT

Signatures for sleptons, which have been extensively studied for the Next Linear Collider, are reexamined taking into account some of the different features of a First Muon Collider.

To appear in *Workshop on Physics at the First Muon Collider and at the Front End of a Muon Collider*, (Fermilab, November 6 – 9, 1997).

This manuscript has been authored under contract number DE-AC02-76CH00016 with the U.S. Department of Energy. Accordingly, the U.S. Government retains a non-exclusive, royalty-free license to publish or reproduce the published form of this contribution, or allow others to do so, for U.S. Government purposes.

Sleptons at a First Muon Collider

Frank E. Paige

*Physics Department
Brookhaven National Laboratory
Upton, NY 11973*

Abstract. Signatures for sleptons, which have been extensively studied for the Next Linear Collider, are reexamined taking into account some of the different features of a First Muon Collider.

Supersymmetry (SUSY) signatures have been extensively studied for the Next Linear Collider (NLC) [1]. The basic strategy [2] [3] uses the fact that SUSY particles are produced in pairs and decay into Standard Model (SM) particles plus an invisible lightest SUSY particle $\tilde{\chi}_1^0$. Hence the maximum and minimum energies of the visible SM particles determine the initial SUSY and LSP mass. However, the NLC studies have used properties of the NLC such as easily variable energy and high electron polarization. This study makes assumptions appropriate for a First Muon Collider (FMC), namely operation at a single energy with a 20° hole for shielding and no polarization. It does not, however, take into account backgrounds from muon decays.

I SLEPTONS AT LHC POINT 5

This analysis is carried out for LHC Point 5, a minimal supergravity (SUGRA) point with $m_0 = 100$ GeV, $m_{1/2} = 300$ GeV, $A_0 = 300$ GeV, $\tan\beta = 2.1$, and $\text{sgn}\mu = +1$. For this point, $M(\tilde{\chi}_1^0) = 121.66$ GeV, $M(\tilde{\ell}_R) = 157.20$ GeV, $M(\tilde{\ell}_L) = 238.82$ GeV, and $M(\tilde{\chi}_{1\pm}) = 232.05$ GeV. The LHC can trivially discover SUSY at this point and can use precision measurements of combination of masses to determine the SUGRA parameters. Using only such precision measurements, the estimated errors for 10 fb⁻¹ of luminosity are [4]

- $m_0 = 100.5^{+12}_{-5}$ GeV,
- $m_{1/2} = 298^{+16}_{-9}$ GeV,
- $\tan\beta = 1.8^{+0.3}_{-0.5}$,

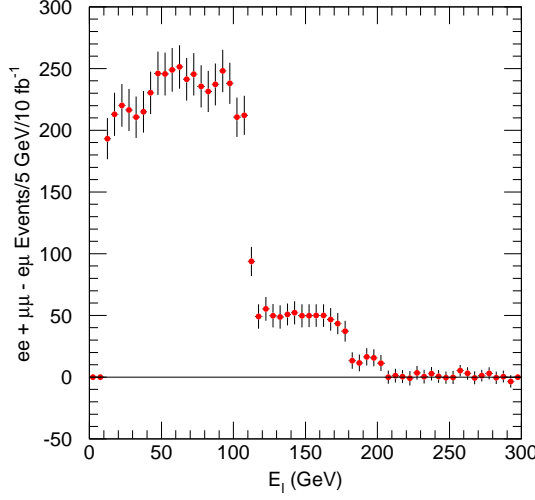


FIGURE 1. The sum of the signal and background for $\mu^+\mu^- + e^+e^- - \mu^\pm e^\mp$ at Point 5 with statistical errors appropriate for 10 fb^{-1} .

- $\text{sgn } \mu = +1$.

A_0 is poorly determined because the weak-scale phenomenology is insensitive to it. The ultimate LHC precision is considerably better [5]. Given these results, one would presumably choose the energy of the FMC to be $\sqrt{s} = 600\text{ GeV}$, the value assumed here.

SUSY and Standard Model events were generated as e^+e^- events with ISAJET 7.31 [6]; e 's and μ 's were interchanged in the analysis. The toy detector simulation is the same as that used for the LHC studies [4] except that the η range is limited to $|\eta| < 1.8$, approximately equivalent to $\theta > 20^\circ$. Jets were found with a fixed cone algorithm, and leptons were taken from the generator. Slepton candidates are selected by requiring two μ or e leptons with $|\eta| < 1.3$ and $E_\ell > 10\text{ GeV}$ and no other leptons or jets. The two leptons are required to satisfy

- $E_\ell > 10\text{ GeV}$, $|\eta_\ell| < 1.3$ to select two identified leptons in the detector,
- $|\vec{p}_1 + \vec{p}_2| < 0.9\sqrt{s}$ to reject lepton pair background,
- $|\vec{p}_{T,1} + \vec{p}_{T,2}| > 10\text{ GeV}$ to reject lepton pair and $\gamma\gamma$ background,
- $\Delta\phi_{1,2} < 0.95\pi$ to reject lepton pair and $\gamma\gamma$ background.

These cuts eliminate the $\ell^+\ell^-$, $\gamma\gamma \rightarrow \ell^+\ell^-$, and $ZZ \rightarrow \ell^+\ell^-\nu\bar{\nu}$ backgrounds. A Z mass cut was found to distort the E_ℓ distributions and was replaced by the cut on $|\vec{p}_{T,1} + \vec{p}_{T,2}|$.

After these cuts, the dominant background comes from leptonic decays of WW pairs. Since W 's decay equally into $e\nu$ and $\mu\nu$, the SM background vanishes up

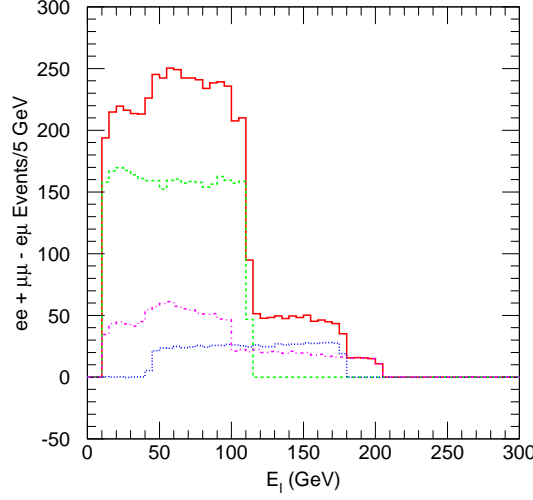


FIGURE 2. Composition of E_ℓ distribution for $\mu^+\mu^- + e^+e^- - e^+\mu^- - e^-\mu^+$ at Point 5. The dashed curve is from $\tilde{\ell}_R\tilde{\ell}_R$; the dotted curve is from $\tilde{\ell}_L\tilde{\ell}_L$; and the dashed-dotted curve is from $\tilde{\ell}_R\tilde{\ell}_L$.

to statistical fluctuations in the combinations $\mu^+\mu^- + e^+e^- - e^+\mu^- - e^-\mu^+$ (and also for $\mu^+\mu^- - e^+e^-$). This distribution is shown in Figure 1 with error bars appropriate for 10 fb^{-1} but with larger Monte Carlo statistics.

The origins of the signal are shown in Figure 2. There are contributions from $\tilde{\ell}_R\tilde{\ell}_R$, $\tilde{\ell}_L\tilde{\ell}_L$, and $\tilde{\mu} +_R \tilde{\mu}_L$, the last coming from gaugino exchange in the t -channel. Two-body kinematics implies that for production of $\tilde{\ell}_i\tilde{\ell}_j$, $i, j = R, L$, the maximum and minimum energies are

$$E_{i \rightarrow \ell}^\pm = \frac{M_i^2 - M_{\tilde{\chi}_1^0}^2}{4M_i^2} \left[\frac{s + M_i^2 - M_j^2 \pm \sqrt{(s - M_i^2 - M_j^2)^2 - 4M_i^2 M_j^2}}{2\sqrt{s}} \right]$$

There are four distinct ranges for the lepton energy, one each for RR and LL events and two for LR events:

$$\begin{aligned} E_{RR} &= (111.4 \text{ GeV}, 11.2 \text{ GeV}) \\ E_{LL} &= (178.3 \text{ GeV}, 33.0 \text{ GeV}) \\ E_{LR} &= (99.5 \text{ GeV}, 10.0 \text{ GeV}) \\ &= (101.9 \text{ GeV}, 19.2 \text{ GeV}) \end{aligned}$$

If no other cuts had been made, one would obtain a sum of four square distributions with these limits. All of these limits can be seen as edges in Figure 2.

The small lower limits for some of these distributions may make it difficult to identify and measure the electrons in the presence of the muon decay background. These limits are an "accidental" consequence of the masses at this point; they decrease slowly as \sqrt{s} is increased.

II ERROR ANALYSIS

The easiest edge to detect in Figure 1 is the one at 111.4 GeV. Statistically, one could detect this with bins of 0.5 GeV, ten times smaller, but detector resolution and possible confusion from the two edges at about 100 GeV must be included. We assume an error $\sigma_E = 1$ GeV. This edge is associated with the ℓ_R sleptons, and its position is given by

$$E_\ell^{\max} = \frac{M_{\ell_R}^2 - M_{\tilde{\chi}_1^0}^2}{4M_{\ell_R}^2} [\sqrt{s} + \sqrt{s - 4M_{\ell_R}^2}]$$

The other RR edge is at such low energy, 11.2 GeV, that it will probably be difficult to measure. The LHC can measure the endpoint of the $\ell^+\ell^-$ mass spectrum and so determine

$$M_{\ell\ell}^{\max} = M_{\tilde{\chi}_{20}} \sqrt{1 - \frac{M_{\ell_R}^2}{M_{\tilde{\chi}_{20}}^2}} \sqrt{1 - \frac{M_{\tilde{\chi}_1^0}^2}{M_{\ell_R}^2}}$$

with an estimated error $\sigma_M = 1$ GeV for 10 fb^{-1} . [4] While one can estimate the masses independently, the results are not so accurate, so we assume $M_{\tilde{\chi}_{20}} = 2M_{\tilde{\chi}_1^0}$. Then the χ^2 error ellipse in the $(M_{\tilde{\chi}_1^0}, M_{\tilde{\ell}_R})$ plane is given by

$$\chi^2 = \sum_{ij} \left[\frac{1}{\sigma_E^2} \frac{\partial E_\ell^{\max}}{\partial M_i \partial M_j} \frac{1}{\sigma_M^2} \frac{\partial M_{\ell\ell}^{\max}}{\partial M_i \partial M_j} \right] \Delta M_i \Delta M_j$$

The resulting error matrix is shown in Figure 3 and represents a significant improvement over the LHC alone.

We next attempt to determine the $\tilde{\ell}_L$ mass by measuring the edge at 178.3 GeV in Figure 1 from $\tilde{\ell}_L^+ \tilde{\ell}_L^-$ production. The error is probably about one bin width, 5 GeV. Unfortunately, the position of this edge,

$$E_\ell^{\max} = \frac{M_{\tilde{\ell}_L}^2 - M_{\tilde{\chi}_1^0}^2}{4M_{\tilde{\ell}_L}^2} [\sqrt{s} + \sqrt{s - 4M_{\tilde{\ell}_L}^2}]$$

turns out to be very insensitive to $M_{\tilde{\ell}_L}$ for these values of the parameters; the derivative of the $\tilde{\ell}_L \tilde{\ell}_L$ endpoint has a zero as a function of \sqrt{s} that happens to occur very close to 600 GeV for these masses. Numerically,

$$\frac{dE_\ell^{\max}}{M_{\tilde{\ell}_L}} \approx 0.036.$$

As a result the sensitivity is accidentally very poor. For "typical" values the error on $M_{\tilde{\ell}_L}$ would be about three times that on the edge.

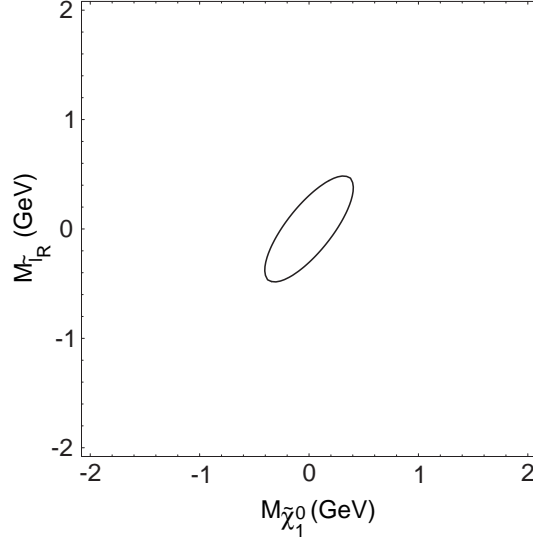


FIGURE 3. Error ellipse in the $(M_{\tilde{\chi}_1^0}, M_{\tilde{\ell}_R})$ plane from measurements at the LHC and FMC at Point 5.

III SLEPTONS AT LHC POINT 3

The second LHC point at which the FMC could contribute is LHC Point 3, a SUGRA point with $m_0 = 200$ GeV, $m_{1/2} = 100$ GeV, $A_0 = 0$, $\tan\beta = 2$, and $\text{sgn}\mu = -1$. These parameters were chosen so that every accelerator could find something; in particular, LEP recently announced discovery of the light Higgs at 68 GeV. The LHC can make many precise measurements at this point. However, since sleptons do not occur in the cascade decays of gluinos and squarks, they are not directly constrained.

Figure 4 shows the lepton energy distribution for Point 3 and its sources; compare with Figure 2 for Point 5. The sleptons are nearly degenerate at this point: $M_{\tilde{\ell}_R} = 206.5$ GeV and $M_{\tilde{\ell}_L} = 215.7$ GeV. Hence all the slepton edges are nearly degenerate; the $\tilde{\ell}_R\tilde{\ell}_R$ contribution dominates because the branching ratio for $\tilde{\ell}_R \rightarrow \tilde{\chi}_1^0\ell$ is nearly 100%. There is also a contribution to like-flavor dileptons from $\tilde{\chi}_1^0$ at this point, the long-dashed curve in Figure 4. While the various contributions in probably cannot be resolved, both the upper and the lower edges should be measurable, allowing one to determine $M_{\tilde{\ell}}$ and $M_{\tilde{\chi}_1^0}$ without additional assumptions. [2] [3] The resulting error ellipse is shown assuming a measurement error of 1 GeV on each edge. Clearly this case is much more favorable than that for Point 5, although in part the difference is due to the fact that there is less information on sleptons from the LHC.

While polarization is not essential to detect the signal, it would help to interpret it. In particular, the dominance of the $\tilde{\ell}_R\tilde{\ell}_R$ contribution seen in Figure 4 is due to $\tilde{\chi}_1^0$ exchange in the t -channel. Even rather modest beam polarization would show that this contribution was dominant and so provide another test of the SUSY model. The degree of polarization required needs study but is probably much smaller than

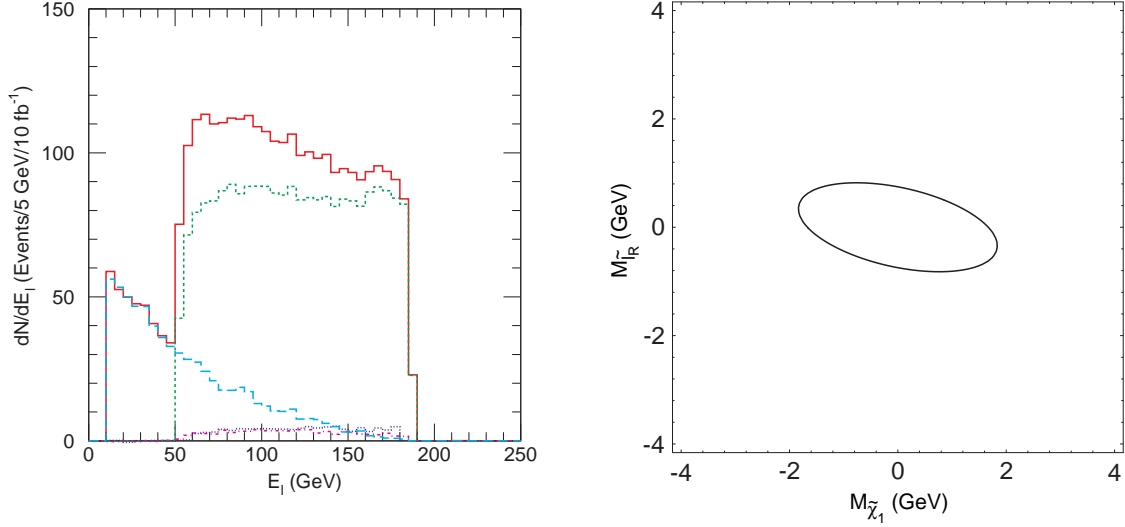


FIGURE 4. Composition of E_ℓ distribution for $\mu^+\mu^- + e^+e^- - e^+\mu^- - e^-\mu^+$ at Point 3. The dashed curve is from $\tilde{\ell}_R\tilde{\ell}_R$; the dotted curve is from $\tilde{\ell}_L\tilde{\ell}_L$; the dashed-dotted curve is from $\tilde{\ell}_R\tilde{\ell}_L$; and the long-dashed curve is from all events with a $\tilde{\chi}20$. The error ellipse is also shown.

that needed to suppress Standard Model backgrounds.

This work was supported in part by the United States Department of Energy under Contract DE-AC02-76CH00016.

REFERENCES

1. S. Kuhlman, et al., *Physics and Technology of the Next Linear Collider*, BNL-52502 (1996)
2. T. Tsukamoto, K. Fujii, H. Murayama, M. Yamaguchi, and Y. Okada, *Phys. Rev.* **D51**, 3153, (1995)
3. M.M. Nojiri, K. Fujii, and T. Tsukamoto *Phys. Rev.* **D54**, 6756 (1996)
4. I. Hinchliffe, M.D. Shapiro, F.E. Paige, J. Soderqvist, W. Yao, *Phys. Rev.* **D55**, 5520 (1997)
5. D. Froidevaux, <http://atlasinfo.cern.ch/Atlas/GROUPS/PHYSICS/SUSY/susy.html>
6. H. Baer, F. Paige, S. Protopopescu and X. Tata; in *Physics at Current Accelerators and Supercolliders*, ed. J. Hewett, A. White and D. Zeppenfeld, (Argonne National Laboratory, 1993).